arXiv:1606.05562v1 [cs.IT] 27 May 2016

An Orthogonal 16-point Approximate DCT for Image and Video Compression

T. L. T. da Silveira* F. M. Bayer† R. J. Cintra‡ S. Kulasekera§
A. Madanayake§ A. J. Kozakevicius¶

Abstract

A low-complexity orthogonal multiplierless approximation for the 16-point discrete cosine transform (DCT) was introduced. The proposed method was designed to possess a very low computational cost. A fast algorithm based on matrix factorization was proposed requiring only 60 additions. The proposed architecture outperforms classical and state-of-the-art algorithms when assessed as a tool for image and video compression. Digital VLSI hardware implementations were also proposed being physically realized in FPGA technology and implemented in 45 nm up to synthesis and place-route levels. Additionally, the proposed method was embedded into a high efficiency video coding (HEVC) reference software for actual proof-of-concept. Obtained results show negligible video degradation when compared to Chen DCT algorithm in HEVC.

Keywords

16-point DCT approximation, Low-complexity transforms, Image compression, Video coding

1 Introduction

The discrete cosine transform (DCT) [1, 2] is a pivotal tool for digital image processing [3–5]. Indeed, the DCT is an important approximation for the optimal Karhunen-Loève transform (KLT), being employed in a multitude of compression standards due to its remarkable energy compaction properties [5–9]. Because of this, the DCT has found at applications in image and video coding

*T. L. T. da Silveira is with the Programa de Pós-Graduação em Informática, Universidade Federal de Santa Maria, Santa Maria, RS, Brazil, thiago@inf.ufsm.br

†F. M. Bayer is with the Departamento de Estatística and LACESM, Universidade Federal de Santa Maria, Santa Maria, RS, Brazil, bayer@ufsm.br

‡R. J. Cintra is with the Signal Processing Group, Departamento de Estatística, Universidade Federal de Pernambuco. E-mail: rjdsc@stat.ufpe.org

§S. Kulasekera and A. Madanayake are with the Department of Electrical and Computer Engineering, University of Akron, Akron, OH, USA, arjuna@uakron.edu

¶A. J. Kozakevicius is with the Departamento de Matemática, Universidade Federal de Santa Maria, Santa Maria, RS, Brazil, alicek@ufsm.br

standards, such as JPEG [10], MPEG-1 [11], MPEG-2 [12], H.261 [13], H.263 [14], and H.264 [15]. Moreover, numerous fast algorithms were proposed for its computation [16–22].

Designing fast algorithms for the DCT is a mature area of research [17, 23–25]; thus it is not realistic to expect major advances by means of standards techniques. On the other hand, the development of low-complexity approximations for DCT is an open field of research. In particular, the 8-point DCT was given several approximations, such as the signed DCT [26], the level 1 DCT approximation [27], the Bouguezel-Ahmad-Swamy (BAS) series of transforms [4, 5, 7, 28, 29], the rounded DCT (RDCT) [8], the modified RDCT [30], the multiplier-free DCT approximation for RF imaging [31], and the improved approximate DCT proposed in [9]. Such approximations reduce the computational demands of the DCT evaluation, leading to low-power consumption and high-speed hardware realizations [9]. At the same time, approximate transforms can provide adequate numerical accuracy for image and video processing.

In response to the growing need for higher compression rates related to real time applications [32], the high efficiency video coding (HEVC) video compression format [33] was proposed. Different from its predecessors, the HEVC employs not only 8×8 size blocks, but also 4×4, 16×16, and 32×32. Several approximations for 16-point DCT based on the integer cosine transform [34] were proposed in [35], [36] and [37]. These transformations are derived from the exact DCT after scaling the elements of the DCT matrix and approximating the resulting real-numbered entries to integers [36]. Therefore, real multiplications can be completely eliminated, at the expense of a noticeable increase in both the additive complexity and the number of required bit-shifting operations [2].

A more restricted class of DCT approximations prescribe transformation matrices with entries defined on the set $\mathcal{C} = \{0, \pm 1/2, \pm 1, \pm 2\}$. Because the elements of $\mathcal{C}$ imply almost null arithmetic complexity, resulting transformations defined over $\mathcal{C}$ have *very* low-complexity, requiring no multiplications and a reduced number of bit-shifting operations. In this context, methods providing 16-point low-cost orthogonal transforms include the Walsh–Hadamard transform (WHT) [38, 39], BAS-2010 [4], BAS-2013 [29], and the approximate transform proposed in [40], here referred to as BCEM approximation. To the best of our knowledge, these are the only 16-point DCT approximations defined over $\mathcal{C}$ archived in literature. Approximations over $\mathcal{C}$ are adequate the HEVC structure [9] and are capable of minimizing the associated hardware power consumption as required by current multimedia market [32].

The aim of this paper is to contribute to image and video compression methods related to JPEG-like schemes and HEVC. Thus, we propose a 16-point approximate DCT, that requires neither multiplications nor bit-shifting operations. Additionally, a fast algorithm is sought, aiming to minimize the overall computation complexity. The proposed transform is assessed and compared with competing 16-point DCT approximations. The realization of the propose DCT approximation in digital VLSI hardware as well as into a HEVC reference software is sought.

This paper unfolds as follows. In Section 2, we propose a new 16-point DCT approximation and

detail its fast algorithm. Section 3 presents the performance analysis of the introduced transformations and compare it to competing tools in terms of the computational complexity coding measures, and similarity metrics with respect to the exact DCT. In Section 4, a JPEG-like image compression simulation is described and results are presented. In Section 5, digital hardware architectures for the proposed algorithm are supplied for both 1-D and 2-D analysis. A practical real-time video coding scenario is also considered: the proposed method is embedded into an open source HEVC standard reference software. Conclusions and final remarks are given in the last section.

2 Proposed transform

Several fast algorithm for the DCT allow recursive structures, for which the computation of the N-point DCT can be split into the computation of $\frac{N}{2}$-point DCT [1, 2, 17, 41–43]. This is usually the case for algorithms based on decimation-in-frequency methods [23, 41].

In account of the above observation and judiciously considering permutations and signal changes, we designed a 16-point transformation that splits itself into two instantiations of the low-complexity matrix associated to the 8-point RDCT [8]. The proposed transformation, denoted as $\mathbf{T}$, is given by:

$$\mathbf{T} = \begin{bmatrix}
1 & 1 & 1 & 1 & 1 & 1 & 1 & 1 & 1 & 1 & 1 & 1 & 1 & 1 & 1 & 1 \\
1 & 1 & 1 & 1 & 1 & 1 & 1 & 1 & -1 & -1 & -1 & -1 & -1 & -1 & -1 & -1 \\
1 & 1 & 1 & 0 & 0 & -1 & -1 & -1 & -1 & -1 & -1 & 0 & 0 & 1 & 1 & 1 \\
1 & 1 & 0 & 0 & 0 & 0 & -1 & -1 & 1 & 1 & 0 & 0 & 0 & 0 & -1 & -1 \\
1 & 0 & 0 & -1 & -1 & 0 & 0 & 1 & 1 & 0 & 0 & -1 & -1 & 0 & 0 & 1 \\
1 & 1 & -1 & -1 & -1 & -1 & 1 & 1 & -1 & -1 & 1 & 1 & 1 & 1 & -1 & -1 \\
1 & 0 & -1 & -1 & 1 & 1 & 0 & -1 & -1 & 0 & 1 & 1 & -1 & -1 & 0 & 1 \\
0 & 0 & -1 & 1 & 1 & -1 & -1 & 1 & -1 & 1 & 1 & -1 & -1 & 1 & 0 & 0 \\
1 & -1 & -1 & 1 & 1 & -1 & -1 & 1 & 1 & -1 & -1 & 1 & 1 & -1 & -1 & 1 \\
1 & -1 & -1 & 1 & 0 & 0 & 1 & -1 & 1 & -1 & 0 & 0 & -1 & 1 & 1 & -1 \\
1 & -1 & 0 & 1 & -1 & 0 & 1 & -1 & -1 & 1 & 0 & -1 & 1 & 0 & -1 & 1 \\
0 & 0 & 1 & 1 & -1 & -1 & 0 & 0 & 0 & 0 & 1 & 1 & -1 & -1 & 0 & 0 \\
0 & -1 & 1 & 0 & 0 & 1 & -1 & 0 & 0 & -1 & 1 & 0 & 0 & 1 & -1 & 0 \\
1 & -1 & 1 & -1 & 1 & -1 & 0 & 0 & 0 & 0 & 1 & -1 & 1 & -1 & 1 & -1 \\
0 & -1 & 1 & -1 & 1 & -1 & 1 & 0 & 0 & 1 & -1 & 1 & -1 & 1 & -1 & 0 \\
1 & -1 & 0 & 0 & -1 & 1 & -1 & 1 & -1 & 1 & -1 & 1 & 0 & 0 & 1 & -1
\end{bmatrix}.$$

Because the entries of $\mathbf{T}$ are in $\{0, \pm 1\} \subset \mathcal{C}$, the proposed matrix is a multiplierless operator. Bit-shifting operations are also unnecessary; only simple additions are required. Additionally, the above matrix obeys the condition: $\mathbf{T} \cdot \mathbf{T}^\top = [\text{diagonal matrix}]$, where superscript $\top$ denotes matrix transposition. Thus, the necessary conditions for orthogonalizing it according to the methods described in [44], [8] and [45] are satisfied. Such procedure yields the following orthogonal 16-point DCT approximation matrix:

$$\hat{\mathbf{C}} = \mathbf{S} \cdot \mathbf{T},$$

where

$$\mathbf{S} = \operatorname{diag}\left(\frac{1}{4}, \frac{1}{4}, \frac{1}{\sqrt{12}}, \frac{1}{\sqrt{8}}, \frac{1}{\sqrt{8}}, \frac{1}{4}, \frac{1}{\sqrt{12}}, \frac{1}{\sqrt{12}}, \right.$$
$$\left. \frac{1}{4}, \frac{1}{\sqrt{12}}, \frac{1}{\sqrt{12}}, \frac{1}{\sqrt{8}}, \frac{1}{\sqrt{8}}, \frac{1}{\sqrt{12}}, \frac{1}{\sqrt{12}}, \frac{1}{\sqrt{12}}\right).$$

In the context of image and video compression, the diagonal matrix $\mathbf{S}$ can be absorbed into the quantization step [4, 5, 7, 8, 25, 45, 46]. Therefore, under these conditions, the complexity of the approximation $\hat{\mathbf{C}}$ can be equated to the complexity of the low-complexity matrix $\mathbf{T}$ [40, 46].

Matrix-based fast algorithm design techniques yield a sparse matrix factorization of $\mathbf{T}$ as given below:

$$\mathbf{T} = \mathbf{P_2} \cdot \mathbf{M_4} \cdot \mathbf{M_3} \cdot \mathbf{M_2} \cdot \mathbf{P_1} \cdot \mathbf{M_1},$$

where

$$\begin{aligned}
\mathbf{M}_1 &= \begin{bmatrix} \mathbf{I}_8 & \bar{\mathbf{I}}_8 \\ \bar{\mathbf{I}}_8 & -\mathbf{I}_8 \end{bmatrix}, \quad \mathbf{P}_1 = \operatorname{diag}\left(\mathbf{I}_9, \begin{bmatrix} 0&0&1&0&0&0&0 \\ 0&0&0&1&0&0&0 \\ 0&0&0&0&0&0&1 \\ 0&0&0&0&0&1&0 \\ 0&0&0&0&1&0&0 \\ 0&1&0&0&0&0&0 \\ 1&0&0&0&0&0&0 \end{bmatrix}\right), \\
\mathbf{M}_2 &= \operatorname{diag}\left(\begin{bmatrix} \mathbf{I}_4 & \bar{\mathbf{I}}_4 \\ \bar{\mathbf{I}}_4 & -\mathbf{I}_4 \end{bmatrix}, \begin{bmatrix} \mathbf{I}_4 & \bar{\mathbf{I}}_4 \\ \bar{\mathbf{I}}_4 & -\mathbf{I}_4 \end{bmatrix}\right), \\
\mathbf{M}_3 &= \operatorname{diag}\left(\begin{bmatrix} 1&0&0&1 \\ 0&1&1&0 \\ 0&-1&1&0 \\ 1&0&0&-1 \end{bmatrix}, \begin{bmatrix} 0&1&1&1 \\ -1&-1&0&1 \\ -1&1&-1&0 \\ 1&0&-1&1 \end{bmatrix}, \begin{bmatrix} 1&0&0&1 \\ 0&1&1&0 \\ 0&-1&1&0 \\ -1&0&0&1 \end{bmatrix}, \begin{bmatrix} 0&1&1&1 \\ 1&1&0&-1 \\ 1&-1&1&0 \\ 1&0&-1&1 \end{bmatrix}\right), \\
\mathbf{M}_4 &= \operatorname{diag}\left(\begin{bmatrix} 1&1 \\ 1&-1 \end{bmatrix}, \mathbf{I}_6, \begin{bmatrix} 1&1 \\ 1&-1 \end{bmatrix}, \mathbf{I}_6\right)
\end{aligned} \tag{1}$$

and matrix $\mathbf{P_2}$ performs the simple permutation (0)(1 8)(2 4 3 11 10 7 12 2)(5 9 13 14 6 5)(15) in cyclic notation [47, p. 77]. Matrices $\mathbf{I}_n$ and $\bar{\mathbf{I}}_n$ denote the identity and counter-identity matrices of order n, respectively.

3 Computational Complexity and Evaluation

In this section, we aim at (i) assessing the computational complexity of the proposed approximation, (ii) evaluating it in terms of approximation error, and (iii) measuring its coding performance [2]. For comparison purposes, we selected the following state-of-the-art 16-point DCT approximations: BAS-2010 [4], BAS-2013 [29] and the BCEM method [40]. We also considered the classical WHT [38] and the exact DCT as computed according to the Chen DCT algorithm [42]. This latter method is the algorithm employed in the HEVC codec by [48].

Table 1: Arithmetic complexity assessment

Transform	Operation count			
	Multiplication	Addition	Bit-shifting	Total
Chen DCT [42]	44	74	0	118
WHT	0	64	0	64
BAS-2010	0	64	8	72
BAS-2013	0	64	0	64
BCEM	0	72	0	72
Proposed	0	**60**	0	**60**

3.1 Arithmetic Complexity

The computational cost of a given transformation is traditionally measured by its arithmetic complexity, i.e, the number of required arithmetic operations for its computation [2,41,49]. Considered operations are multiplications, additions, and bit-shifting operations [41]. Table 1 lists the operation count for each arithmetical operation for all considered methods. Total operation count is also provided.

The proposed transform showed 6.25% less total operation count when compared with the WHT or BAS-2013 approximation. Considering BAS-2010 or the BCEM approximation, the introduced approximation required 16.67% less operation overall. As a more strict complexity assessment, even if we take only the additive complexity into account, the proposed transformation can still outperform all considered methods. It is also noteworthy that the proposed method has the lowest multiplicative complexity among all considered methods. Moreover, to the best of our knowledge, the proposed transformation outperforms any meaningful 16-point DCT approximation archived in literature.

3.2 Similarity Measures

For the approximation error analysis, we considered three tools: the DCT distortion [50], the total error energy [8], and the mean square error (MSE) [1, 2]. This set of measures determines the similarity between the exact DCT matrix and a given approximation. These quality metrics are briefly described as follows.

Let $\mathbf{C}$ be the exact N-point DCT matrix and $\tilde{\mathbf{C}}$ be a given N-point DCT approximation. Adopting the notation employed in [37], the DCT distortion of $\tilde{\mathbf{C}}$ is given by:

$$d_2(\tilde{\mathbf{C}}) = 1 - \frac{1}{N} \cdot \left\| \mathrm{diag}\left(\mathbf{C} \cdot \tilde{\mathbf{C}}^\top\right) \right\|^2,$$

where $\| \cdot \|$ is the Euclidean norm [51]. The DCT distortion captures the difference between the exact DCT matrix and a candidate approximation by quantifying the orthogonality among the

basis vectors of both transforms [37].

Taking the basis vectors of the exact DCT and a given approximation as filter coefficients, the total error energy [8], measures the spectral proximity between the corresponding transfer functions [26]. Invoking Parseval theorem [52], the total error energy can be evaluated according to:

$$\epsilon(\tilde{\mathbf{C}}) = \pi \cdot \left\| \mathbf{C} - \tilde{\mathbf{C}} \right\|_{\mathrm{F}}^{2},$$

where $\| \cdot \|_{\mathrm{F}}$ is the Frobenius norm [51].

The MSE is a well-established proximity measure [2]. The MSE between $\mathbf{C}$ and $\tilde{\mathbf{C}}$ is given by [2, 24]:

$$\mathrm{MSE}(\tilde{\mathbf{C}}) = \frac{1}{N} \cdot \mathrm{tr}\left((\mathbf{C} - \tilde{\mathbf{C}}) \cdot \mathbf{R} \cdot (\mathbf{C} - \tilde{\mathbf{C}})^{\top} \right),$$

where $\mathrm{tr}(\,\cdot\,)$ is the trace function [53] and $\mathbf{R}$ is the covariance matrix of the input signal. Assuming the first-order stationary Markov process model for the input data, we have that $\mathbf{R}_{[i,j]} = \rho^{|i-j|}$, for $i, j = 1, 2, \ldots, N$, and the correlation coefficient ρ is set to 0.95 [2, 24]. This particular model is suitable for real signals and natural images [2, 24, 45]. The minimization of MSE values indicates proximity to the exact DCT [2].

3.3 Coding Measures

We adopted two coding measures: the transform coding gain [37] and the transform efficiency [2]. The transform coding gain quantifies the coding or data compression performance of an orthogonal transform [2, 37]. This measure is given by [2, 54]:

$$C_g(\tilde{\mathbf{C}}) = 10 \cdot \log_{10} \left\{ \frac{\frac{1}{N} \sum_{i=0}^{N-1} s_{ii}}{\left[\prod_{i=0}^{N-1} \left(s_{ii} \cdot \sqrt{\sum_{j=0}^{N-1} \tilde{\mathbf{c}}_{ij}^{2}} \right) \right]^{\frac{1}{N}}} \right\},$$

where s_{ij} and $\tilde{\mathbf{c}}_{ij}$ are the (i, j)-th entry of $\tilde{\mathbf{C}} \cdot \mathbf{R} \cdot \tilde{\mathbf{C}}^{\top}$ and $\tilde{\mathbf{C}}$, respectively.

On the other hand, the transform efficiency [2] is an alternative method to compute the compression performance. Denoted by η, the transform efficiency is furnished by:

$$\eta(\tilde{\mathbf{C}}) = \frac{\sum_{i=0}^{N-1} |s_{ii}|}{\sum_{i=0}^{N-1} \sum_{j=0}^{N-1} |s_{ij}|} \times 100.$$

Quantity $\eta(\tilde{\mathbf{C}})$ indicates the data decorrelation capability of the transformation. The KLT achieves optimality with respect to this measure, presenting a transform efficiency of 100 [2].

Table 2: Performance analysis

Transform	Measures				
	Approximation			Coding	
	d_2	ϵ	MSE	C_g	η
DCT	0	0	0	9.4555	88.4518
WHT	0.8783	92.5631	0.4284	8.1941	70.6465
BAS-2010	0.6666	64.749	0.1866	**8.5208**	**73.6345**
BAS-2013	0.5108	54.6207	0.132	8.1941	70.6465
BCEM	**0.1519**	**8.0806**	**0.0465**	7.8401	65.2789
Proposed	**0.3405**	**30.323**	**0.0639**	**8.295**	**70.8315**

3.4 Results

Table 2 summarizes the results for the above detailed similarity and coding measures. For each figure of merit, we emphasize in bold the two best measurements. The proposed transform displays consistently good performance according to all considered criteria. This fact contrasts with existing transformations, which tend to excel in terms of similarity measures, but perform limitedly in terms of coding performance; and vice-versa. Therefore, the proposed transform offers a compromise, while still achieving state-of-the-art performance.

4 Application to image compression

The proposed approximation was submitted to the image compression simulation methodology originally introduced in [26] and employed in [4, 5, 7, 8, 29, 40]. In our experiments a set of 45 512×512 8-bit grayscale images obtained from a standard public image bank [55] was considered to validate the proposed algorithm. We adapted the JPEG-like compression scheme for the 16×16 matrix case, as suggested in [4].

The adopted image compression method is detailed as follows. An input 512×512 image was divided into 16×16 disjoint blocks $\mathbf{A}_k$, $k = 0, 1, \ldots, 31$. Each block $\mathbf{A}_k$ was 2-D transformed according to $\mathbf{B}_k = \tilde{\mathbf{C}} \cdot \mathbf{A}_k \cdot \tilde{\mathbf{C}}^\top$, where $\mathbf{B}_k$ is a frequency domain image block and $\tilde{\mathbf{C}}$ is a given approximation matrix. Matrix $\mathbf{B}_k$ contains the 256 transform domain coefficients for each block. Adapting the zigzag sequence [56] for the 16×16 case, we retained only the r initial coefficients and set the remaining coefficients to zero [4, 5, 7, 8, 26, 29, 40], generating $\mathbf{B'}_k$. Subsequently, the inverse transformation was applied to $\mathbf{B'}_k$ according to: $\mathbf{A'}_k = \tilde{\mathbf{C}}^\top \cdot \mathbf{B'}_k \cdot \tilde{\mathbf{C}}$. The above procedure was repeated for each block. The rearrangement of all blocks $\mathbf{A'}_k$ reconstructs the image, which can be assessed for quality.

Image degradation was evaluated using two different quality measures: (i) the peak signal-to-noise ratio (PSNR) and (ii) the structural similarity index (SSIM) [57]—a generalization of the

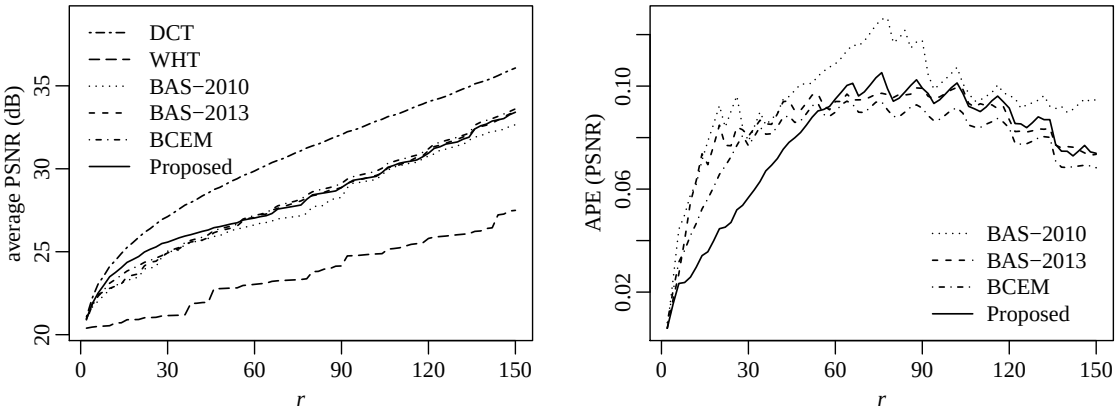

(a) Average PSNR

(b) Absolute percentage error of PSNR

Figure 1: PSNR results for all considered transforms under several compression rates

universal image quality index [58]. In contrast to the PSNR, SSIM definition takes advantage of known characteristics of the human visual system [57]. Following the methodology adopted in [8] and [40], we calculated average PSNR and SSIM values for all 45 images.

Fig. 1(a) and Fig. 2(a) show average PSNR and SSIM measurements, respectively. Additionally, we considered absolute percentage error (APE) measurements of PSNR and SSIM with respect to the exact DCT. Results are displayed in Fig. 1(b) and Fig. 2(b), for PNSR and SSIM, respectively. APE figures for the WHT are absent because their values were exceedingly high, being located outside of the plot range.

According to Figs. 1 and 2, the proposed transform outperforms other methods for $r \leq 50$, which correspond to high-compression rates. Therefore, the proposed transform is in consonance with ITU recommendation for high-compression coding in real time applications [32]. For $r > 50$, discussed methods are essentially comparable in terms of image degradation.

As a qualitative comparison, Fig. 3 shows the compressed *Lena* image at $r = 16$ (93.75% compression) obtained from each considered method. The proposed transform offered less pixelation and block artifacts; demonstrating its adequacy for high-compression rate scenarios.

5 Digital Architecture and Realization

In this section, hardware architectures for the proposed 16-point approximate DCT are detailed. Both 1-D and 2-D transformations are addressed. Introduced architectures were submitted to (i) Xilinx field programmable gate array (FPGA) implementations and (ii) CMOS 45 nm application specific integrated circuit (ASIC) implementation up to the synthesis level. Additionally, in order to assess the performance of the proposed algorithm in real time video coding, the introduced approximation was also embedded into an HEVC reference software [59].

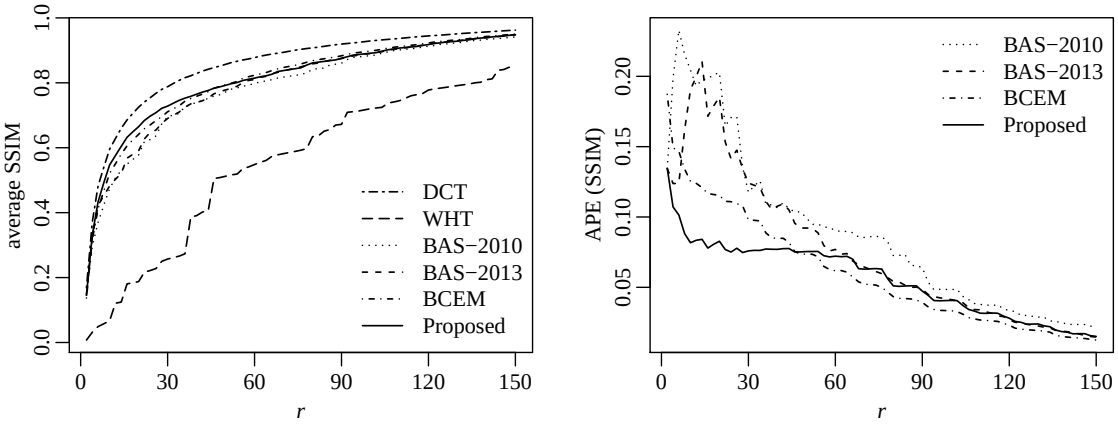

(a) Average SSIM

(b) Absolute percentage error of SSIM

Figure 2: SSIM results for all considered transforms under several compression rates

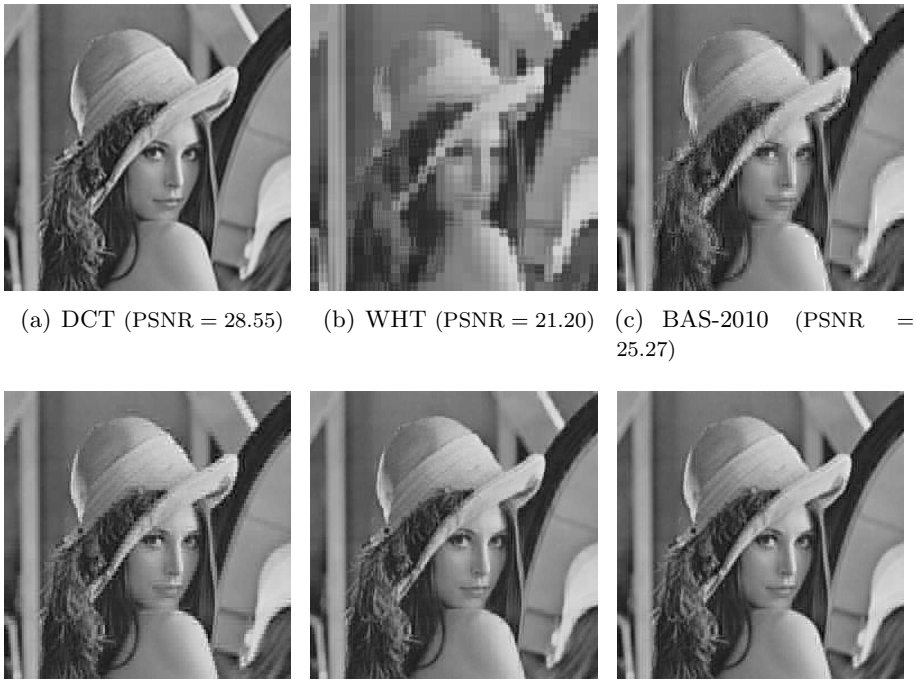

(a) DCT (PSNR = 28.55)

(b) WHT (PSNR = 21.20)

(c) BAS-2010 (PSNR = 25.27)

(d) BAS-2013 (PSNR = 25.79)

(e) BCEM (PSNR = 25.75)

(f) Proposed (PSNR = 27.13)

Figure 3: Compressed *Lena* image using all considered transforms, for $r = 16$

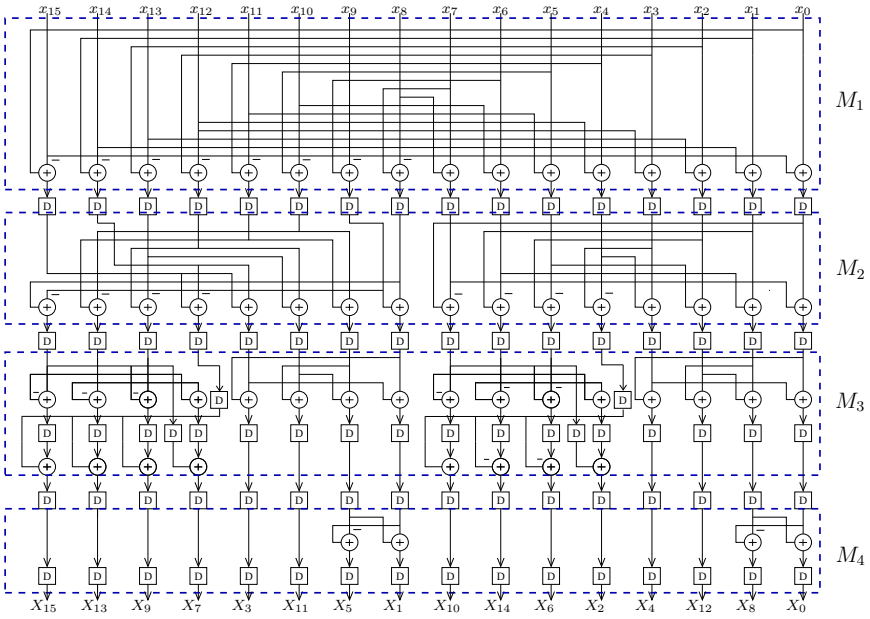

Figure 4: Architecture of the proposed 16-point DCT approximation

5.1 Architecture for the 16-point DCT approximation

The 2-D version of the 16-point DCT approximation architecture was realized using two 1-D transforms and a transpose buffer. This is possible because the proposed approximation inherits the separable kernel property of the exact DCT [60]. The first instantiation of the approximate DCT block furnishes a row-wise transform computation of the input image, while the second implementation furnishes a column-wise transformation of the previous intermediate result. A real time row-parallel transposition buffer circuit is required in between the 1-D transformation blocks. Such block ensures data ordering for converting the row-transformed data from the first DCT approximation circuit to a transposed format as required by the second DCT approximation circuit. Both 1-D transformation blocks and the transposition buffer were initially modeled and tested in Matlab Simulink; then they were combined to furnish the complete 2-D approximate transform. Fig. 4 depicts the architecture for the proposed 1-D approximate DCT. We emphasize in dashed boxes the blocks M_1, M_2, M_4, and M_4, which correspond to the realization of sparse matrices $\mathbf{M_1}$, $\mathbf{M_2}$, $\mathbf{M_3}$, and $\mathbf{M_4}$, respectively, as shown in the equation set (1). Fig. 5 shows the implementation of the 2-D transform by means of the 1-D transforms.

5.2 FPGA and ASIC realizations and results

The above discussed architecture was physically realized on a FPGA based rapid prototyping system for various register sizes and tested using on-chip hardware-in-the-loop co-simulation. The architecture was designed for digital realization within the MATLAB environment using the Xilinx

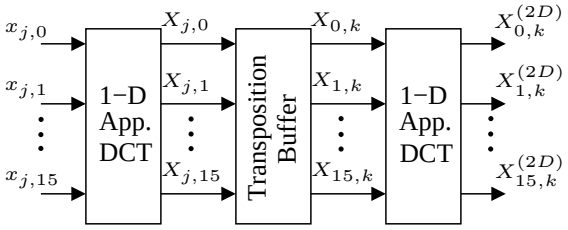

Figure 5: Two-dimensional approximate transform by means of 1-D approximate transform. Signal $x_{k,0}, x_{k,1}, \ldots$, corresponds to the rows of the input image; $X_{k,0}, X_{k,1}, \ldots$ indicates the transformed rows; $X_{0,j}, X_{1,j}, \ldots$ indicates the columns of the transposed row-wise transformed image; and $X_{0,j}^{(2\text{-D})}, X_{1,j}^{(2\text{-D})}, \ldots$ indicates the columns of the final 2-D transformed image

Table 3: Hardware resource consumption and power consumption for the proposed 2-D 16-point DCT approximation

CLB	FF	T_{cpd} (ns)	$F_{\max}$ (MHz)	D_p (mW/MHz)	Q_p (W)
1408	4600	3.7	270.27	6.91	3.481

System Generator. Xilinx Virtex-6 XC6VLX240T-1FFG1156 device was employed to physically realize the architecture on FPGA with fine-grain pipelining for increased throughput. The realization was verified on FPGA chip using a Xilinx ML605 board at a clock frequency of 50 MHz. The FPGA realization was tested with 10,000 random 16-point input test vectors using hardware co-simulation. Test vectors were generated from within the MATLAB environment and routed to the physical FPGA device using JTAG based hardware co-simulation. Then measured data from the FPGA was routed back to MATLAB memory space.

Evaluation of hardware complexity and real time performance considered the following metrics: the number of used configurable logic blocks (CLB), flip-flop (FF) count, critical path delay (T_{cpd}), and the maximum operating frequency ($F_{\max}$) in MHz. The `xflow.results` report file was accessed to obtain the above results. Dynamic (D_p) and static power (Q_p) consumptions were estimated using the Xilinx XPower Analyzer. Results are shown in Table 3.

For the ASIC implementation, the hardware description language code was ported to 45 nm CMOS technology and subject to synthesis and place-and-route steps using the Cadence Encounter. The FreePDK, a free open-source ASIC standard cell library at the 45 nm node, was used for this purpose. The supply voltage of the CMOS realization was fixed at $V_{\text{DD}} = 1.1$ V during estimation of power consumption and logic delay. The adopted figures of merit for the ASIC synthesis were: area (A) in mm^2, area-time complexity (AT) in mm$^2 \cdot$ ns, area-time-squared complexity (AT^2) in mm$^2 \cdot$ns^2, dynamic (D_p) power in (mW/MHz) and static (Q_p) power consumption in watts, critical path delay (T_{cpd}) in ns, and maximum operating frequency ($F_{\max}$) in MHz. Results are displayed in Table 4.

Among the considered competitors, the BAS-2010 [4] showed arithmetic complexity and coding

Table 4: Hardware resource consumption for CMOS 45nm ASIC place-route implementation of the proposed 2-D 16-point DCT approximation

Area$_{(\mathrm{mm}^2)}$	AT	AT^2	T_{cpd}(ns)	$F_{\max}$(MHz)	D_p(mW/MHz)	Q_p(mW)
0.585	4.896	40.98	8.37	119.47	0.311	216.2

Table 5: Hardware resource consumption of the 1-D approximations using Xilinx Virtex-6 XC6VLX240T-1FFG1156 device

Transform	CLB	FF	T_{cpd} (ns)	$F_{\max}$ (MHz)	D_p (mW/MHz)	Q_p (W)
BAS-2010	430	1440	1.950	512.82	4.54	3.49
Proposed	421	1372	1.900	526.31	4.22	3.49

performance similar to the proposed transform. For comparison purposes the 1-D versions of the BAS-2010 approximation and the proposed 16-point approximation were realized on a Xilinx Virtex-6 XC6VLX240T-1FFG1156 device as well as were ported to 45 nm CMOS technology and subject to synthesis and place-and-route steps using the Cadence Encounter. The results are shown in Table 5 and Table 6. Compared to the BAS-2010, the proposed transform is faster when both the FPGA implementation and CMOS synthesis is considered while having similar performance in hardware usage and dynamic power consumption. Importantly, the proposed is better in image quality as evidenced by Fig. 3.

5.3 Real time video compression software implementation

In order to assess real-time video coding performance, the proposed approximation was embedded into the open source HEVC standard reference software by the Fraunhofer Heinrich Hertz Institute [59]. The original transform prescribed in the selected HEVC reference software is the scaled approximation of Chen DCT algorithm [42, 48] and the software can process image block sizes of 4×4, 8×8, 16×16, and 32×32.

Our methodology consists of replacing the 16×16 DCT algorithm of the reference software by the proposed 16-point approximate algorithm. Algorithms were evaluated for their effect on the overall performance of the encoding process. For such, we obtained rate-distortion (RD) curves for

Table 6: Hardware resource consumption for CMOS 45nm ASIC place-route implementation of the 1-D approximations

Transform	Area$_{(\mathrm{mm}^2)}$	AT	AT^2	$T_{\mathrm{cpd}(\mathrm{ns})}$	$F_{\max(\mathrm{MHz})}$	$D_{p(\mathrm{mW/MHz})}$	$Q_{p(\mathrm{mW})}$
BAS-2010	0.169	0.843	4.21	4.994	200.24	0.093	70.47
Proposed	0.183	0.895	4.38	4.895	204.29	0.095	78.73

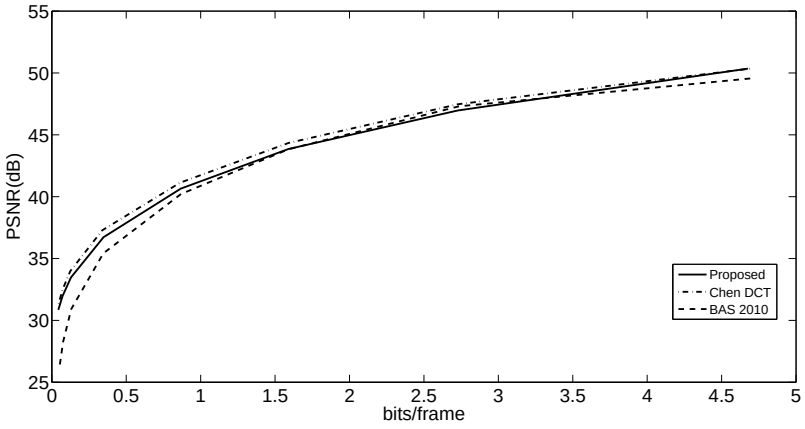

Figure 6: RD curves for 'BasketballPass' test sequence

standard video sequences [61]. The quantization point (QP) varied from 0 to 50 to obtain the curves and the resulting PSNR values with the bit rate values measured in bits per frame were recorded for the proposed algorithm, the Chen DCT algorithm, and the BAS-2010 [4] algorithm. Fig. 6 depicts the obtained RD curves for the 'BasketballPass' test sequence. Fig. 7 shows particular 416×240 frames for the test video sequence 'BasketballPass' with QP $\in \{0, 32, 50\}$.

The RD curves and selected frames reveal that the difference between the original HEVC and the implementation with the proposed approximation is negligible. In fact, in Fig. 6 the maximum PSNR difference is 0.56 dB, which is very low. Fig. 7 shows that both encoded video streams are almost identical. These results confirm the adequacy of the proposed scheme.

6 Conclusion

This work proposed a new orthogonal 16-point DCT approximation. The introduced transform offers a very low computational cost, outperforming—to the best of our knowledge—all competing methods. Moreover, the proposed transform performed well as an image compression tool, specially at high compression rate scenarios. By means of (i) comprehensive computational simulations, (ii) hardware implementation (both in FPGA and ASIC), and (iii) software embedding, we demonstrated the adequacy and efficiency of the proposed method, which is suitable for codec schemes, like the HEVC. Additionally, the introduced transformation offers an unusual good performance balance among several metrics, as shown in Table 2. This suggests that the applicability of proposed transform is not limited in scope to the image and video compression context.

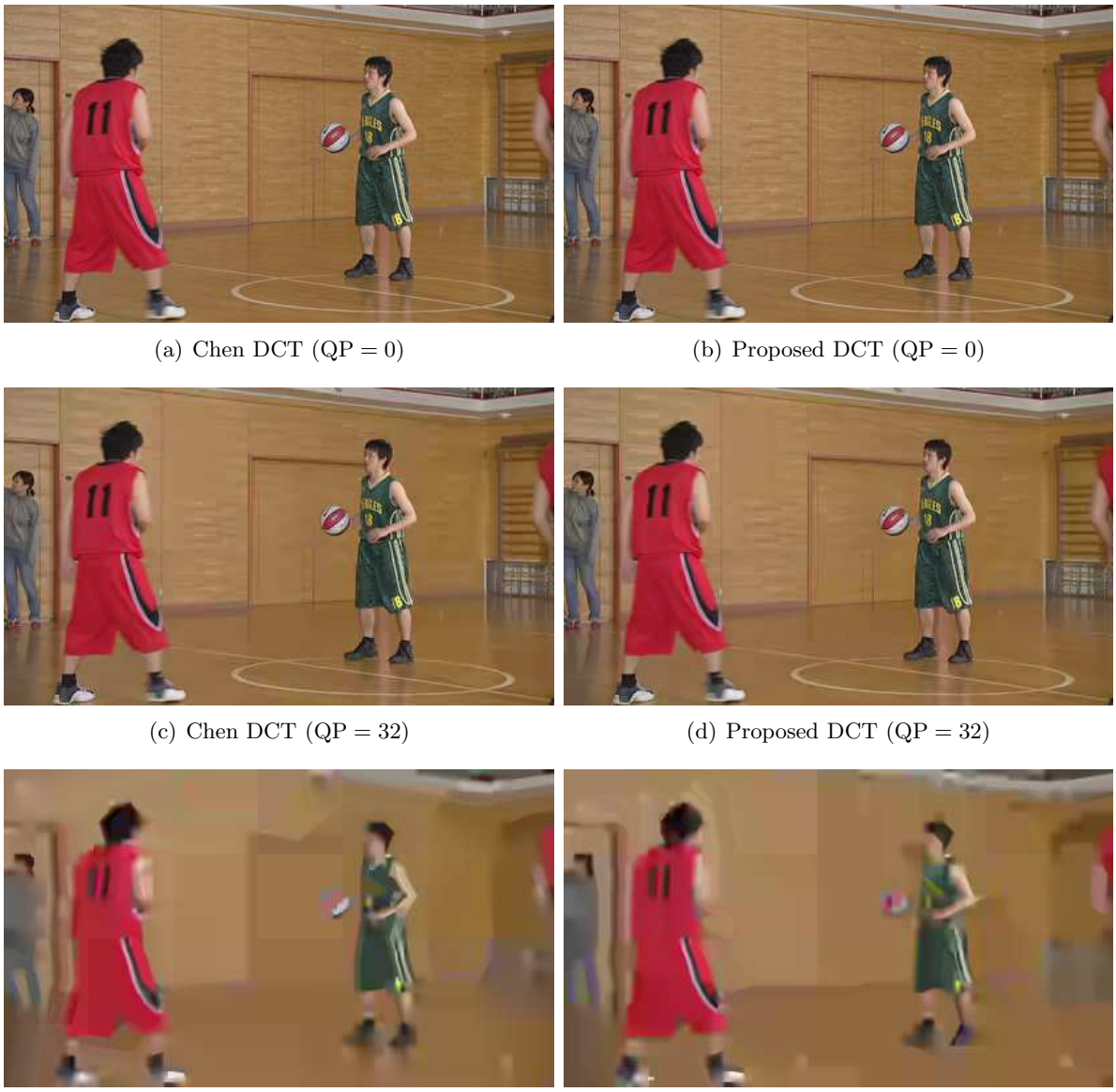

(a) Chen DCT (QP = 0)

(b) Proposed DCT (QP = 0)

(c) Chen DCT (QP = 32)

(d) Proposed DCT (QP = 32)

(e) Chen DCT (QP = 50)

(f) Proposed DCT (QP = 50)

Figure 7: Selected frames from 'BasketballPass' test video coded by means of the Chen DCT and the proposed 16-point DCT approximation for QP = 0 (a–b), QP = 32 (c–d), and QP = 50 (e–f)

Acknowledgments

This work was partially supported by CPNq, FACEPE, FAPERGS and FIT/UFSM (Brazil), and by the College of Engineering at the University of Akron, Akron, OH, USA.

References

[1] K. R. Rao and P. Yip, *Discrete Cosine Transform: Algorithms, Advantages, Applications*. San Diego, CA: Academic Press, 1990.

[2] V. Britanak, P. Yip, and K. R. Rao, *Discrete Cosine and Sine Transforms*. Academic Press, 2007.

[3] M. C. Lin, L. R. Dung, and P. K. Weng, "An ultra-low-power image compressor for capsule endoscope," *BioMedical Engineering OnLine*, vol. 5, no. 1, pp. 1–8, Feb. 2006.

[4] S. Bouguezel, M. O. Ahmad, and M. N. S. Swamy, "A novel transform for image compression," in *53rd IEEE International Midwest Symposium on Circuits and Systems (MWSCAS)*, Aug. 2010, pp. 509–512.

[5] ——, "A Low-Complexity Parametric Transform for Image Compression," in *Proceedings of the 2011 IEEE International Symposium on Circuits and Systems*, 2011.

[6] T.-S. Chang, C.-S. Kung, and C.-W. Jen, "A simple processor core design for DCT/IDCT," *IEEE Transactions on Circuits and Systems for Video Technology*, vol. 10, no. 3, pp. 439–447, Apr 2000.

[7] S. Bouguezel, M. O. Ahmad, and M. N. S. Swamy, "Low-complexity 8×8 transform for image compression," *Electronics Letters*, vol. 44, no. 21, pp. 1249–1250, Sep. 2008.

[8] R. J. Cintra and F. M. Bayer, "A DCT approximation for image compression," *IEEE Signal Processing Letters*, vol. 18, no. 10, pp. 579–582, Oct. 2011.

[9] U. S. Potluri, A. Madanayake, R. J. Cintra, F. M. Bayer, S. Kulasekera, and A. Edirisuriya, "Improved 8-point approximate DCT for image and video compression requiring only 14 additions," *IEEE Transactions on Circuits and Systems I*, vol. 61, no. 6, pp. 1727–1740, 2014.

[10] W. B. Pennebaker and J. L. Mitchell, *JPEG Still Image Data Compression Standard*. New York, NY: Van Nostrand Reinhold, 1992.

[11] N. Roma and L. Sousa, "Efficient hybrid DCT-domain algorithm for video spatial downscaling," *EURASIP Journal on Advances in Signal Processing*, vol. 2007, no. 2, pp. 30–30, 2007.

[12] International Organisation for Standardisation, "Generic coding of moving pictures and associated audio information – Part 2: Video," ISO, ISO/IEC JTC1/SC29/WG11 - Coding of Moving Pictures and Audio, 1994.

[13] International Telecommunication Union, "ITU-T recommendation H.261 version 1: Video codec for audiovisual services at $p \times 64$ kbits," ITU-T, Tech. Rep., 1990.

[14] ——, "ITU-T recommendation H.263 version 1: Video coding for low bit rate communication," ITU-T, Tech. Rep., 1995.

[15] Joint Video Team, "Recommendation H.264 and ISO/IEC 14 496–10 AVC: Draft ITU-T recommendation and final draft international standard of joint video specification," ITU-T, Tech. Rep., 2003.

[16] Y. Arai, T. Agui, and M. Nakajima, "A fast DCT-SQ scheme for images," *Transactions of the IEICE*, vol. E-71, no. 11, pp. 1095–1097, Nov. 1988.

[17] C. Loeffler, A. Ligtenberg, and G. Moschytz, "Practical fast 1D DCT algorithms with 11 multiplications," in *Proceedings of the International Conference on Acoustics, Speech, and Signal Processing*, 1989, pp. 988–991.

[18] Z. Wang, "Fast algorithms for the discrete W transform and for the discrete Fourier transform," *IEEE Transactions on Acoustics, Speech and Signal Processing*, vol. ASSP-32, pp. 803–816, Aug. 1984.

[19] B. G. Lee, "A new algorithm for computing the discrete cosine transform," *IEEE Transactions on Acoustics, Speech and Signal Processing*, vol. ASSP-32, pp. 1243–1245, Dec. 1984.

[20] M. Vetterli and H. Nussbaumer, "Simple FFT and DCT algorithms with reduced number of operations," *Signal Processing*, vol. 6, pp. 267–278, Aug. 1984.

[21] H. S. Hou, "A fast recursive algorithm for computing the discrete cosine transform," *IEEE Transactions on Acoustic, Signal, and Speech Processing*, vol. 6, no. 10, pp. 1455–1461, 1987.

[22] E. Feig and S. Winograd, "Fast algorithms for the discrete cosine transform," *IEEE Transactions on Signal Processing*, vol. 40, no. 9, pp. 2174–2193, 1992.

[23] M. T. Heideman and C. S. Burrus, *Multiplicative complexity, convolution, and the DFT*, ser. Signal Processing and Digital Filtering. Springer-Verlag, 1988.

[24] J. Liang and T. D. Tran, "Fast multiplierless approximation of the DCT with the lifting scheme," *IEEE Transactions on Signal Processing*, vol. 49, pp. 3032–3044, 2001.

[25] A. Edirisuriya, A. Madanayake, V. Dimitrov, R. J. Cintra, and J. Adikari, "VLSI architecture for 8-point AI-based Arai DCT having low area-time complexity and power at improved accuracy," *Journal of Low Power Electronics and Applications*, vol. 2, no. 2, pp. 127–142, 2012.

[26] T. I. Haweel, "A new square wave transform based on the DCT," *Signal Processing*, vol. 82, pp. 2309–2319, 2001.

[27] K. Lengwehasatit and A. Ortega, "Scalable variable complexity approximate forward DCT," *IEEE Transactions on Circuits and Systems for Video Technology*, vol. 14, no. 11, pp. 1236–1248, Nov. 2004.

[28] S. Bouguezel, M. O. Ahmad, and M. Swamy, "A fast 8×8 transform for image compression," in *2009 International Conference on Microelectronics (ICM)*, Dec. 2009, pp. 74–77.

[29] S. Bouguezel, M. O. Ahmad, and M. N. S. Swamy, "Binary discrete cosine and Hartley transforms," *IEEE Transactions on Circuits and Systems I: Regular Papers*, vol. 60, no. 4, pp. 989–1002, 2013.

[30] F. M. Bayer and R. J. Cintra, "DCT-like transform for image compression requires 14 additions only," *Electronics Letters*, vol. 48, no. 15, pp. 919–921, 2012.

[31] U. S. Potluri, A. Madanayake, R. J. Cintra, F. M. Bayer, and N. Rajapaksha, "Multiplier-free DCT approximations for RF multi-beam digital aperture-array space imaging and directional sensing," *Measurement Science and Technology*, vol. 23, no. 11, p. 114003, 2012.

[32] International Telecommunication Union, *Infrastructure of audiovisual services - Coding of moving video - High efficiency video coding.* Telecommunication Standarization Sector of ITU, 2013.

[33] M. T. Pourazad, C. Doutre, M. Azimi, and P. Nasiopoulos, "HEVC: The new gold standard for video compression: How does HEVC compare with H.264/AVC?" *IEEE Consumer Electronics Magazine*, vol. 1, no. 3, pp. 36–46, Jul. 2012.

[34] W. K. Cham, "Development of integer cosine transforms by the principle of dyadic symmetry," in *IEE Proceedings I Communications, Speech and Vision*, vol. 136, no. 4, 1989, pp. 276–282.

[35] W. K. Cham and Y. T. Chan, "An order-16 integer cosine transform," *IEEE Transactions on Signal Processing*, vol. 39, no. 5, pp. 1205–1208, 1991.

[36] J. Dong, K. N. Ngan, C.-K. Fong, and W.-K. Cham, "2-D order-16 integer transforms for HD video coding," *IEEE Transactions on Circuits and Systems for Video Technology*, vol. 19, no. 10, pp. 1462–1474, 2009.

[37] C.-K. Fong and W.-K. Cham, "LLM integer cosine transform and its fast algorithm," *IEEE Transactions on Circuits and Systems for Video Technology*, vol. 22, no. 6, pp. 844–854, 2012.

[38] R. K. Yarlagadda and J. E. Hershey, *Hadamard Matrix Analysis and Synthesis With Applications to Communications and Signal/Image Processing*. Kluwer Academic Publishers, 1997.

[39] I. Valova and Y. Kosugi, "Hadamard-based image decomposition and compression," *IEEE Transactions on Information Technology in Biomedicine*, vol. 4, no. 4, pp. 306–319, 2000.

[40] F. M. Bayer, R. J. Cintra, A. Edirisuriya, and A. Madanayake, "A digital hardware fast algorithm and FPGA-based prototype for a novel 16-point approximate DCT for image compression applications," *Measurement Science and Technology*, vol. 23, no. 8, pp. 114 010–114 019, 2012.

[41] R. E. Blahut, *Fast Algorithms for Signal Processing*. Cambridge University Press, 2010.

[42] W. H. Chen, C. Smith, and S. Fralick, "A fast computational algorithm for the discrete cosine transform," *IEEE Transactions on Communications*, vol. 25, no. 9, pp. 1004–1009, Sep. 1977.

[43] P. Yip and K. R. Rao, "The decimation-in-frequency algorithms for a family of discrete sine and cosine transform," *Circuits, Systems, and Signal Processing*, pp. 4–19, 1988.

[44] R. J. Cintra, "An integer approximation method for discrete sinusoidal transforms," *Circuits, Systems, and Signal Processing*, vol. 30, no. 6, pp. 1481–1501, 2011.

[45] R. J. Cintra, F. M. Bayer, and C. J. Tablada, "Low-complexity 8-point DCT approximations based on integer functions," *Signal Processing*, vol. 99, pp. 201–214, 2014.

[46] T. D. Tran, "The binDCT: Fast multiplierless approximation of the DCT," *IEEE Signal Processing Letters*, vol. 6, no. 7, pp. 141–144, 2000.

[47] I. N. Herstein, *Topics in Algebra*, 2nd ed., W. India, Ed. John Wiley & Sons, 1975.

[48] M. Capelo, "Advances on transforms for high efficiency video coding," Master's thesis, Instituto Superior Técnico, Lisboa, 2011.

[49] J. G. Proakis and D. K. Manolakis, *Digital Signal Processing*, 4th ed. Prentice Hall, 2006.

[50] M. Wien and S. Sun, "ICT comparison for adaptive block transforms," Tech. Rep., 2001.

[51] D. S. Watkins, *Fundamentals of Matrix Computations*, ser. Pure and Applied Mathematics: A Wiley Series of Texts, Monographs and Tracts. Wiley, 2004.

[52] A. V. Oppenheim, *Discrete-Time Signal Processing*. Pearson Education, 2006.

[53] G. A. F. Seber, *A Matrix Handbook for Statisticians*. Wiley-Interscience, 2007.

[54] H. S. Malvar, *Signal Processing with Lapped Transforms*. Artech House, 1992.

[55] "The USC-SIPI image database," http://sipi.usc.edu/database/, 2011, University of Southern California, Signal and Image Processing Institute.

[56] I.-M. Pao and M.-T. Sun, "Approximation of calculations for forward discrete cosine transform," *IEEE Transactions on Circuits and Systems for Video Technology*, vol. 8, no. 3, pp. 264–268, Jun. 1998.

[57] Z. Wang, A. C. Bovik, H. R. Sheikh, and E. P. Simoncelli, "Image quality assessment: from error visibility to structural similarity," *IEEE Transactions Image Processing*, vol. 13, no. 4, pp. 600–612, Apr. 2004.

[58] Z. Wang and A. Bovik, "A universal image quality index," *IEEE Signal Processing Letters*, vol. 9, no. 3, pp. 81–84, 2002.

[59] Joint Collaborative Team on Video Coding (JCT-VC), "HEVC references software documentation," 2013, Fraunhofer Heinrich Hertz Institute. [Online]. Available: https://hevc.hhi.fraunhofer.de/

[60] S. W. Smith, *The Scientist & Engineer's Guide to Digital Signal Processing*, 1997.

[61] A. Ortega and K. Ramchandran, "Rate-distortion methods for image and video compression," *IEEE Signal Processing Magazine*, vol. 15, no. 6, pp. 23–50, Nov 1998.